The parameters of Mg/Fe(Al) layered double hydroxides/mixed oxides related to the synthesis

Karel Frolich[1], Zdeněk Tišler[2], Jáchym Mück[1]*,
and Lenka Skuhrovcová[2]

[1] *Department of Physical Chemistry,*
The University of Pardubice, CZ–532 10 Pardubice, Czech Republic
[2] *Orlen UniCRE, CZ–436 70 Záluží - Litvínov, Czech Republic*

The Mg-Fe layered double hydroxides (LDH) are becoming to be a group of promising materials with a lot of applications depending on their properties. These are influenced by the methods of synthesis, where it is not clearly presented which synthesis is suitable for materials with desired parameters. The aim of this work was to synthesize MgFe LDH according to standard recipes used for common MgAl LDH, when showing similarities and differences in-between the samples of Mg-Al and Mg-Fe LDH and derived mixed oxides (MO). Extensive experimental characterization of material structure and surface has been performed. Originally, statistical analysis of the characterization data revealed that LDH from particular synthesis were grouped together, showing statistical similarities. The structure properties of samples from particular synthesis were similar to both series of Mg/Al and Mg/Fe and also for the molar metal ratios 3/1 and 4/1. Oxides were completely rehydrated to the LDH form only for the co-precipitation method. The cell parameters in LDH and rehydrated forms mutually strongly correlated indicating the same layer properties of parent LDH and their rehydrated forms. The oxides that originated from the hydrothermal method had significantly higher densities of basic centres and population of strong O^{2-} basic structures due to the abundance of surface defects and other phases. Oxides prepared by the sol-gel method showed somewhat higher density of the acid centres.

Keywords: Layered double hydroxide; Mixed oxide; Synthesis; Structure; Acidobasicity

---

*   Corresponding author, ✉ jachym.muck@student.upce.cz

Introduction

Hydrotalcite is a natural mineral belonging to the group of layered double hydroxides (LDH). This group of significant materials has found many applications in last years in magnetization, biomedical science, environmental chemistry, and catalysis. Solid-like heterogeneous catalysts based on LDH provide opportunities for environmentally friendly organic syntheses [1–4]. LDH-based materials are versatile catalysts due to their tunable basic properties, by selection of divalent or trivalent metal cations and their ratio, anion exchange ability (direct or oxide rehydration), and particularly, by the synthesis method (whether co-precipitation, urea method, hydrothermal or sol-gel) [3,5–7]. Mg/Al and Mg/Fe LDH and related mixed oxides (MO) catalyse chemical reactions, such as aldol condensation, Knoevenagel condensation, transesterification of oils, and others [8–19]. The physicochemical properties that are managed by the synthesis decide about the final application. Therefore, understanding of the dependence between chemical-physical properties and a method of synthesis is important.

Chemical composition of LDH is represented by the general formula $[M^{2+}_{1-x} M^{3+}_{x} (OH)_2]^{x+} [(A^{n-})_{x/n} \cdot yH_2O]^{x-}$ where M^{2+} and M^{3+} are divalent and trivalent cations with similar dimensions as Mg^{2+}. The presence of different cations is generally associated with differences in the physicochemical properties of the material. The presence of M^{3+} cations generates positive charge, which is compensated by anions, mostly carbonates [5,20]. The latter may be more or less successfully replaced by other anions, such as chlorides, nitrates, sulfates or anions of organic acids. Anion exchange is a typical property of hydrotalcites and similar materials [21–23]. Materials are characterized by a layered structure derived from brucite. In the structure of brucite, chemically $Mg(OH)_2$, magnesium ions are octahedrally coordinated by hydroxyl groups. These octahedral fragments form two-dimensional sheets, layers, via edge sharing and may stack together by hydrogen bonding between the hydroxyl groups of adjacent sheets. At sufficiently high temperature, LDH decompose, water and carbon dioxide escape, and a more or less homogeneous MO is then formed. The MO derived from hydrotalcite materials have a mesoporous structure, a high specific surface area, varying basic properties with the presence of strongly basic oxygen, often formed on defects of a more-or-less disordered layered mixed oxide structure [24,25]. A specific property of such mixed oxides is the ability to rehydrate, partially or completely, and reversely transformation into the LDH phase [26–28].

LDH can be prepared by several different methods. Easy and often used is the co-precipitation method [5,29,30], where inorganic salt solutions are co-precipitated in an alkaline solution of hydroxide or carbonate, alkali itself or ammonia [31–33] under well-defined conditions, such as temperature, pH and vigorous stirring. A relatively slow hydrolysis of urea at particular temperature relates to the constant pH and results in the formation of well crystallized hydrotalcite-like products.

Another synthesis is the sol-gel method [34,35]. Herein, the metal precursor – most often an organic compound (e.g., an alkoxide) – is dissolved and hydrolysed in water or an organic solvent. For poorly soluble salts, a suitable solvent and/or higher temperature are to be selected. Yet another route of preparing LDH is hydrothermal synthesis. Hydrothermal synthesis can be a modification of the co-precipitation method or the urea hydrolysis method [36–39]. For badly crystalizing reagents, it is possible to utilize hydrothermal synthesis in an autoclave at temperatures above the boiling point of the solvent and below the decomposition temperature of hydrotalcites.

This paper focuses on the preparation of MgFe LDH and MO with nominal Mg^{2+}/Fe^{3+} ratios with 3 and 4 by standard recipes previously determined for MgAl (co-precipitation and sol-gel approach). The aim was to explore possible differences in the synthesized LDH, namely the presence of another phase, crystallinity, particle size, and temperature stability. The possibility to apply the hydrothermally modified urea method for synthesis of MgFe LDH is also tested. Important features of related MO are probed – specific surface area and pore size distribution, concentration, density and distribution of acidic and basic centres, as well as memory effect (reconstruction to hydrotalcite) are also examined. All such information is relevant for application of LDH and MO as catalysts in selected catalysed reactions. The purpose of the paper is to compare MgFe and MgAl materials prepared by these different methods in one place, the parameters of which are selected on the basis of available studies and own tests, and to define their main similarities and differences. The statistical analysis was used for the description and explanation of mutual relationships among the LDH properties. Principal component analysis (PCA) was carried out and component weight plots (CWP) applied.

Materials and methods

Material synthesis and treatment

For each synthesis of LDH used in this contribution, there were previously described variable reaction conditions: (i) co-precipitation method [24–26,28], (ii) sol-gel method [25,34,35,40], and (iii) hydrothermal method [37,41,42]. Conditions for the individual synthesis with the LDH phase formation were selected based on literature data, our experience, and as such are presented below. The synthesis methods were described mostly for MgAl LDH (hydrotalcite-like materials). Chosen synthesis conditions were applied in the synthesis of Mg/Fe LDH, which have not been studied so far.

The co-precipitation method was performed in a precipitation reactor made of Syrris Globe glass (Syrris, Royston, UK). A solution of Mg^{2+}, Al^{3+} (or Fe^{3+}) cations were prepared by dissolving the respective nitrate hydrates in deionized

water in a molar ratio of Mg^{2+}/Me^{3+} = 3 or 4 and at a concentration of cations 1 mol dm^{-3}. The stock solution was prepared by dissolving potassium carbonate and potassium hydroxide in deionized water (c_{KOH} = 2 mol dm^{-3}; $c_{K_2CO_3}$ = 0.2 mol dm^{-3}). Deionized water (1 dm^3) was put to the reactor and heated up to 60 °C under stirring. The nitrate solution was then dosed into the reactor at a rate of 30 cm^3 min^{-1} and the stock solution continually added at a rate of 50 cm^3 min^{-1} while stirring at 250 rpm. The dosing of solutions was controlled by pH maintained at 9.5. After the addition of the coprecipitation agent, the solution was left for 1 hour and then the suspension formed was filtered on a laboratory filter press fitted by Hobrafilt S15N filter plates (Hobra – Školník, Broumov, Czech Republic). The product was washed on the filter with distilled water until the neutral reaction of the filtrate (at pH 7). The filtered product was dried at 65 °C for 12 hours. Materials prepared by the co-precipitation method are denoted generally co-LDH, and particularly co-Mg/Al(Fe)-*X*, where *X* denotes theoretical metal ratio.

The sol-gel method was performed in a two-necked glass flask with reflux condenser with a temperature-controlled stirrer. The magnesium ethoxide was dissolved in ethanol (99.8%) to obtain a concentration of 0.75 mol dm^{-3}. A nitric acid solution (40%) was dropwise added until the pH 3. The solution was then heated under reflux for 3 hours while stirring. Subsequently, an acetone solution of Al^{3+} (Fe^{3+}) acetylacetonate (0.25 mol dm^{-3}) was then added, respecting a molar ratio of Mg^{2+}/Me^{3+} = 3 or 4. The pH of the mixture was adjusted (10) by slow dropwise addition of aqueous ammonia solution (33%) and the solution was brought to boiling (at 80 °C) and maintained under stirring for 12 hours or until a gel was forming. Lastly, the gel was filtered and washed several times with distilled water until the pH dropped to 7 and then dried at 65 °C for 12 hours. Materials prepared by the sol-gel method are denoted generally sg-LDH, and particularly sg-Mg/Al(Fe)-*X*, where *X* denotes theoretical metal ratio.

The synthesis of materials by hydrothermal method was performed in an autoclave Versoclave 1.0lt (Büchi Labortechnik AG, Flawil, Switzerland). Molar ratios of Mg-Al(Fe) LDH with a Mg/Al(Fe) = 3 and 4 were prepared by dissolving the appropriate amount of the respective nitrate hydrates and urea in distilled water (c_{urea} = 1.4 mol dm^{-3}). The solution (750 cm^3) was quantitatively transferred to an autoclave. The preparation of hydrotalcite was carried out at 180 °C with vigorous stirring (400 rpm) for 2 hours. Subsequently, the reaction mixture was cooled to 60 °C and the solid was collected by filtration and washed twice with distilled water until pH 7. Finally, the solid phase was allowed to dry at 65 °C for 12 hours. Materials prepared hydrothermally are denoted generally hl-LDH, and particularly hl-Mg/Al(Fe)-*X*, where *X* is theoretical metal ratio.

The MO were obtained by calcination of the prepared LDH in an electric muffle furnace at temperature 450/500°C MgAl/MgFe LDH. The temperature program was set in both cases to a temperature gradient of 5 °C min^{-1} from RT to

450 °C (500 °C) followed by the isotherm for 3 hours. MO prepared by the decomposition of LDH are denoted generally co(sg or hl)-MO, and particularly co(sg or hl)-MO-Mg/Al(Fe)-*X*, where *X* means theoretical metal ratio.

The rehydration of the MO was attempted ex-situ. 1.5 g of MO was put into 22.5 cm^3 of demineralized water. The suspension was stirred at room temperature for 1 hour in a beaker with a magnetic bar at 100 rpm. The slurry was then filtered through a Büchner funnel through a filter paper (390 type). The material was further dried in a flow of nitrogen for 1 hour (vacuum rotary evaporator, 50 °C, atmospheric pressure; Steinberg Systems, Köpenicker, Germany). Prepared materials are generally denoted co(sg or hl)-reMO, and particularly co(sg or hl)-reMO-Mg/Al(Fe)-*X*, where *X* represents theoretical metal ratio.

Characterization

The chemical composition was determined by the LDH prepared. The analysis was performed on an ICP OES Agilent 725 (Agilent Technologies, Santa Clara, CA, USA). Prior to analysis, a 500 mg sample was weighed and Mg-Al LDH was dissolved in 10 cm^3 of H_2SO_4 (50%) and Mg-Fe LDH in 10 cm^3 HCl (31%) at increased temperature. After dissolution, the solution was cooled, diluted with demineralized water and reheated to 100 °C for a few minutes. The solution was transferred to a volumetric flask and measured.

The crystallographic structure of synthesized materials was determined by X-ray powder diffraction on a D8 Advance ECO unit (Bruker Corporation, Billerica, MA, USA) with Cu-Kα radiation (λ = 1.5406 Å). Measurement was done in 2θ range of 5–70 ° with a step size of 0.02 ° and a step time of 0.5 s. Diffractograms were evaluated in the Diffrac.Eva program with a powder diffraction database (PDF 4 2018, ICDD). The crystallite size of LDH was determined by Scherer equation from diffraction line at 2 theta 11° [43]. The cell parameters *a* and *c* were calculated from diffraction lines corresponds to (110) and (003) diffraction planes by equations *a* = 2*d*(110) and *c* = 3*d*(003).

Mass-to-temperature changes were determined for prepared LDH and reMO by thermogravimetric measurements performed on a TGA Discovery instrument (TA Instruments, New Castle, DE, USA). Approximately 15 mg of the sample was weighed into an open corundum crucible. The measurement was performed at a temperature gradient of 10 °C min^{-1} from 40 °C to 900 °C under a flow of nitrogen (20 cm^3 min^{-1}; Linde 5.0, Linde Group, Dublin, Ireland).

Specific surface area (evaluated by BET method) and pore size distribution (evaluated by NLDFT method) was performed by nitrogen absorption/desorption at −196 °C on an Autosorb iQ device (Quantachrome Corporation, Graz, Austria). The prepared LDH were dried in a glass cell at 110 °C, MO at 200 °C, under vacuum for 16 hours before assay.

SEM images were obtained with a scanning electron microscope Lyra3 GMU (Tescan Orsay Holding, Brno, Czech Republic). The samples were mounted on a holder and dusted on a Q150R ES unit (Quorum Technologies, Judges House, UK). The respective images of the samples were obtained at an accelerating voltage of 12 kV over a current range of 200 to 300 pA. For imaging, SE detection was used to examine the sample morphology.

The measurements of CO_2 and NH_3 TPD curves were performed on an Autochem II 2920 analyzer (Micromeritics Instrument Corporation, Norcross, GA, USA). Approximately 100 mg of sample was weighed into a U-tube reactor and heated at 10 °C min^{-1} in helium (99.999%) to 450 °C (Mg/Al) or 500 °C (Mg/Fe) and pretreated at this temperature for 5 min. Then, the sample was cooled down to 35 °C (NH_3-TPD – 70 °C) and helium stream switched to $(NH_3)CO_2$/He mixture. The sample was saturated by CO_2/NH_3 for 30 minutes and the gas was then switched back to helium, when weakly adsorbed CO_2/NH_3 molecules were removed for 60 minutes at 35/70 °C. TPD curves were obtained by increasing the temperature from 35/70 °C to 900 °C with a temperature gradient of 10 °C/min. Changes in gas concentration were monitored using an OmniStarTM GSD320 MS instrument (Pfeiffer Vacum, Ablar, Germany).

Results and discussion

Chemical composition

Both Mg/Al and Mg/Fe LDH were synthesized with a theoretical metal molar ratio of 3/1 and 4/1. The ICP-OES technique was used to determine the real metal content, resp. metal ratio, in the prepared materials (see Table 1). It is evident that in the case of co-LDH the theoretical and real metal content in the materials do not differ much, the highest deviation is observed in the sample co-Mg/Al-3, in which the real ratio is by 3.7 % higher than the theoretical one. This is in consent with the literature that the divalent cations have better ability to be built into the structure of LDH, than that of trivalent cations. The difference between theoretical and real molar ratio of LDH could also be caused by the different content of hydrated water bonded in metal nitrates used for synthesis [44–46]. In contrast, sg-LDH showed slightly higher deviations, namely in the case of samples sg-Mg/Fe-3/1 and sg-Mg/Fe-4/1 the deviation is up to 8 %, in both directions. The highest deviations in the metal ratio could be observed for hl-LDH, where sample hl-Mg/Al-3 had the real ratio by about 28 % higher than that of the theoretical. The higher differences between the theoretical and real molar ratio of metals in the hydrothermal preparation method could be related to the presence of other crystallographic phases next to LDH (chapter Crystallographic structure). Thus, it can be stated that the co-precipitation method leads to the samples with the metal contents closest to the target values.

Table 1 Chemical composition of prepared LDH

Sample	Mg [wt.%]	Al [wt.%]	Fe [wt.%]	Mg^{2+}/Me^{3+} [–]
co-Mg/Al-3	25.50	9.11	–	3.11
co-Mg/Al-4	19.80	5.54	–	3.97
co-Mg/Fe-3	22.90	–	17.60	2.99
co-Mg/Fe-4	24.70	–	14.30	3.97
hl-Mg/Al-3	29.20	8.47	–	3.83
hl-Mg/Al-4	25.30	6.40	–	4.39
sg-Mg/Al-3	23.80	8.70	–	3.04
sg-Mg/Fe-3	21.90	–	18.20	2.76
sg-Mg/Fe-4	24.00	–	12.80	4.31

Crystallographic structure

The crystallographic structure of all studied materials was studied using powder XRD. The corresponding diffractograms for parent LDH, MO and reMO are depicted in Fig. 1, Fig. 2 and Fig. 3, respectively. The values of cell parameters *a*, *c* and crystallite sizes *D* for LDH and corresponding MO are presented in Table 2.

The diffractograms of the parent LDH (Fig. 1) contain lines at $2\theta \approx 11.0$; 22.5; 34.5; 38.0; 44.0; 60.5; 60.9 °, typical for the LDH. The structures prepared by co-precipitation and sol-gel method contained only LDH lines as pure hydrotalcite-like phases were synthesized by these methods. The obtained values of cell parameter *a* (Table 2) are in accordance with published values for pure hydrotalcites Mg/Al (0.305 nm) and pyroaurites Mg/Fe (0.311 nm) [5,18,43,47]. In contrast, hydrothermal prepared samples contained additional diffraction lines. For hl-LDH-Mg/Al, the portion of LDH phase was around 70 %, and additional magnesite and hydromagnesite phases observed at 9.65 ° (PDF 25-0513). Also, the values of cell parameter *a* for hl-LDH-Mg/Al were slightly lower compared to pure hydrotalcite phase (0.305 nm). For hl-LDH-Mg/Fe, the presence of LDH phase was not observed, samples contained only magnesite and hematite phases. Here, we can conclude that Mg/Fe LDH cannot be prepared by the hydrothermal method under the set of synthesis conditions. Therefore, hl-LDH-Mg/Fe is not considered further in this work.

The hydrothermal method leads to the LDH with the highest values of crystallite sizes (60–70 nm). Co-precipitation and sol-gel method give rise to significantly lower crystallite sizes, 10–15 nm (co-LDH) and 9–10 nm (sg-LDH). This finding is in agreement with the previous results [40,47]. In hydrothermal method, aging and an increase in crystallinity occur at high temperatures during the last hour of the reaction, when small LDH crystals dissolve and reprecipitate

to form a much more crystalline product by the Ostwald ripening process [48]. In addition, the LDH with $Mg^{2+}/Me^{3+} = 3$ reveal a slightly higher crystallite sizes in comparison with LDH with $Mg^{2+}/Me^{3+} = 4$.

The diffractograms for the calcined LDH, resultant MO forms (Fig. 2) contain diffraction lines at $2\theta \approx 43.6$ and 62.2 ° representing magnesium oxide (periclase). The presence of MgO proves that during the calcination the layered structure of parent LDH decomposes and the MO form. Oxides originated from co-precipitation and sol-gel do not contain additional phases next to the homogeneous mixed Mg/Al and Mg/Fe oxide. The products from hydrothermal synthesis differ from each other, the hl-MO-Mg/Al-3 does not contain any additional phase, and, in contrast, hl-MO-Mg/Al-4 possess a dominant magnesite phase.

For all materials after rehydration process, the corresponding diffractograms are depicted in Fig. 3. Diffraction lines characteristic for LDH are observed, which means that the layered structure has been restored, either partially or completely. The respective values of cell parameters a and c (Table 2) also support the occurrence of rehydration. In the co-precipitation method, for co-reMO-Mg/Al, a multiple increase in peak intensities is observed compared to the parent LDH due to the formation of a more ordered LDH phase after rehydration. A significant increase in the crystallite sizes is observed for co-reMO-Mg/Al compared to the parent co-LDH-Mg/Al (Table 2). In the case of co-reMO-Mg/Fe, comparable peak intensities are observed as in the original LDH and crystallite sizes are also comparable. All co-precipitated samples were therefore completely (reversibly) rehydrated to the LDH form. In the sol-gel method, after rehydration, the peak intensities of the respective sg-reMO-Mg/Al and sg-reMO-Mg/Fe decrease compared to the parent LDH. For all sg-reMO samples, additional diffraction lines typical for MgO (periclase) appear in the diffractograms, which indicates that the rehydration was not carried out in a 100 % degree for sol-gel prepared MO. Crystallite sizes of sg-reMO have shown somewhat lower values compared to the parent sg-LDH. In the hydrothermal method, hl-MO-Mg/Al-3 was almost completely rehydrated to the LDH form, and heterogeneous hl-MO-Mg/Al-4 sample partially rehydrated being characterized by about 71 % of the LDH phase. Finally, crystallite sizes of hl-reMO were ascertained markedly lower compared to the parent hl-LDH.
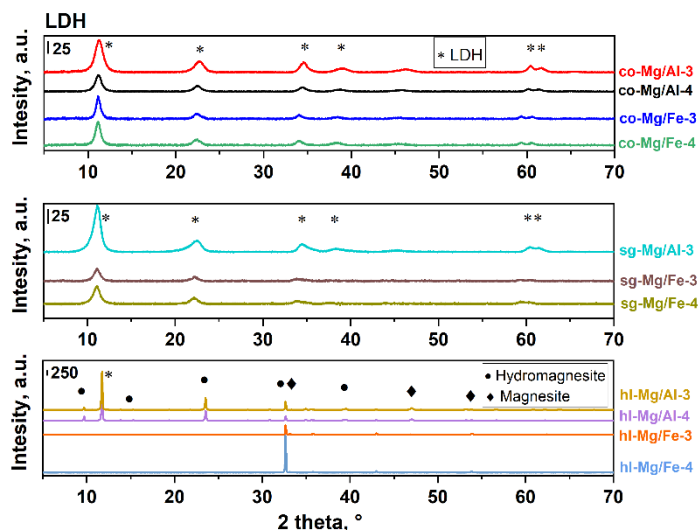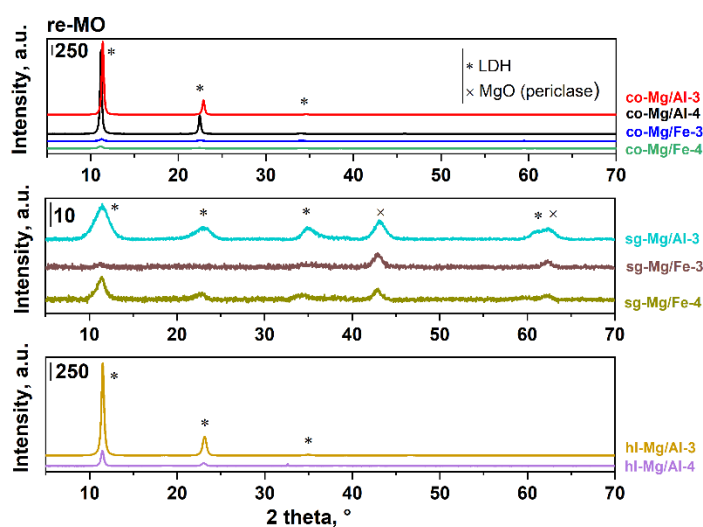
Fig. 1 Diffractograms of parent LDH
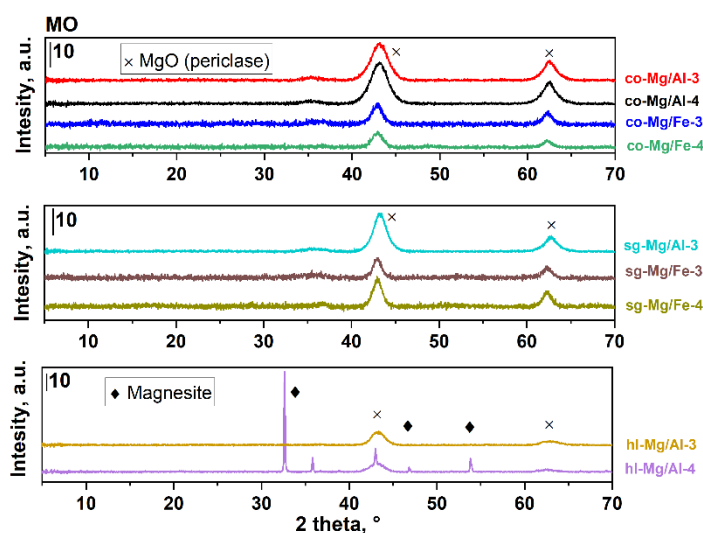
**Fig. 2** Diffractograms of MO

Fig. 3 Diffractograms of reMO

Table 2 Unit cell parameters for parent LDH and related reMO

Sample	LDH			reMO		
	a [nm]	c [nm]	D [nm]	a [nm]	c [nm]	D [nm]
co-Mg/Al-3	0.305	2.340	14.2	0.308	2.378	34.6
co-Mg/Al-4	0.307	2.371	9.6	0.308	2.378	37.4
co-Mg/Fe-3	0.311	2.376	15.6	0.311	2.341	19.6
co-Mg/Fe-4	0.311	2.352	11.1	0.311	2.341	15.3
sg-Mg/Al-3	0.306	2.377	8.6	0.313	1.566	4.9
sg-Mg/Fe-3	0.311	2.386	10.1	–	–	–
sg-Mg/Fe-4	0.311	2.394	9.7	0.313	1.566	9.0
hl-Mg/Al-3	0.304	2.267	66.3	0.304	2.270	25.5
hl-Mg/Al-4	0.304	2.260	61.8	0.305	2.270	23.7

Temperature stability

The temperature dependence of the weight loss and the temperature dependence of the weight-loss derivation were monitored by TG analysis. TGA and dTGA curves of synthesized parent LDH and reMO are depicted in Fig. 4 and 5, respectively. The temperature maxima and related weight losses are summarized in Table 3 and 4. Using TGA curves and derived dTGA curves, it is possible to explore changes in the temperature stability among the studied syntheses, the parent LDH and reMO, and further Mg/Al and Mg/Fe series.
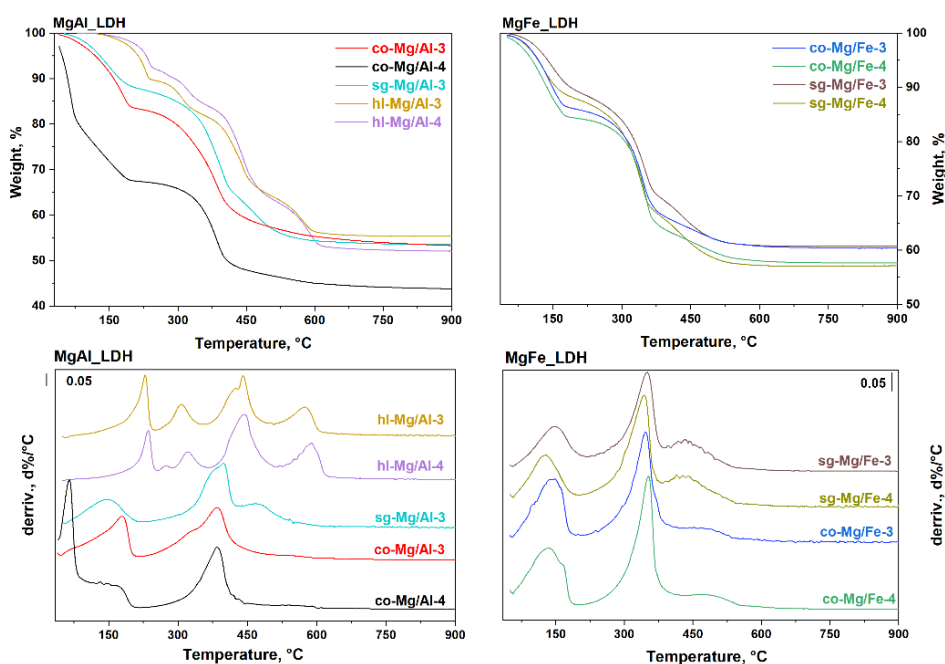
Fig. 4 TGA (up) and dTGA (down) curves of parent LDH

Table 3 Determination of the temperature maximum and weight loss in TGA of the LDH

sample	T_{max} [°C]	Weight loss [wt.%]	T_{max} [°C]	Weight loss [wt.%]	T_{max} [°C]	Weight loss [wt.%]	T_{max} [°C]	Weight loss [wt.%]	T_{max} [°C]	Weight loss [wt.%]
co-Mg/Fe-3	145	13.92	–	–	–	–	347	21.09	–	6.60
co-Mg/Fe-4	135	15.42	–	–	–	–	352	22.52	–	4.50
co-Mg/Al-3	180	16.59	–	–	–	–	385	26.31	–	1.76
co-Mg/Al-4	166	32.58	–	–	–	–	385	19.79	–	2.47
sg-Mg/Al-3	145	12.08	–	–	–	–	399	23.66	468	9.99
sg-Mg/Fe-3	148	11.38	–	–	–	–	349	19.03	433	8.51
sg-Mg/Fe-4	127	11.92	–	–	–	–	343	22.50	432	4.50
hl-Mg/Al-3	229	10.50	–	–	307	5.09	441	20.61	574	7.89
hl-Mg/Al-4	235	7.96	274	4.15	322	6.42	443	17.85	589	10.65

Table 4 Determination of the temperature maximum and weight loss in TGA of the reMO

| sample	T_{max} [°C]	Weight loss [wt.%]	T_{max} [°C]	Weight loss [wt.%]	T_{max} [°C]	Weight loss [wt.%]	T_{max} [°C]	Weight loss [wt.%]
co-Mg/Fe-3	73	11.11	124	15.95	359	14.37	–	2.98
co-Mg/Fe-4	63	5.86	119	17.89	373	16.72	–	3.32
co-Mg/Al-3	–	–	180	14.62	436	25.95	–	–
co-Mg/Al-4	111	54.81	–	–	416	16.73	–	–
sg-Mg/Al-3	–	–	133	12.28	362	14.58	–	–
sg-Mg/Fe-3	88	2.54	144	3.97	311	4.72	–	3.28
sg-Mg/Fe-4	–	–	115	13.47	313	10.17	–	3.42
hl-Mg/Al-4	107	49.65	167	7.79	411	10.56	–	–
hl-Mg/Al-3	75	20.41	214	8.51	371	14.38	–	–

Two dominant steps can be observed in both TGA and dTGA curves for measured LDH and reMO originated from the co-precipitation and sol-gel methods. In the first step (at a temperature of 50–200 °C), physically adsorbed water and water bound in the anionic layer evaporates. In the second step (at a temperature of 200–500 °C), water is produced from the dehydroxylation of brucite-like sheets and carbon dioxide from the decomposition of interlayer carbonates [5]. In the case of LDH and reMO from the hydrothermal modified urea method, the decomposition of the structure is more complex, characterized by additional separated steps/maxima. The weight loss for hl-LDH relates, next to the loss of water and carbon dioxide, also to the decomposition of residual urea, and for higher temperatures compounds derived from urea in the interlayer.

Co-precipitated LDH and reMO with Mg/Al-3 have the first maximum around 180–185 °C, Mg/Al-4 between 60–110 °C, the second maximum is between 380–440 °C for both ratios. For the co-precipitated Mg/Fe samples, the first maximum is between 130–140 °C, the second between 340–370 °C. Co-precipitated reMO have shifted maxima to higher temperatures compared to the parent LDH. For co-reMO Mg/Fe there is also an additional peak between 65–75 °C.

Sol-gel prepared LDH and reMO reveal the first maximum between 110–150 °C, the second maximum around 320–400 °C. For the parent sg-LDH, the third maximum between 330–370 °C is also evident. The maxima in sg-reMO are slightly shifted to lower temperatures than in the case of parent sg-LDH. The second maximum is significantly lower in intensity for sg-reMO compared to the parent sg-LDH. Sg-reMO-Mg/Fe-3 has maxima with a very low intensity.

Hydrothermally prepared LDH and reMO reveal more complex curves compared to the other synthesis methods. The first maximum for hl-LDH is observed in the range of 229–235 °C, which is a significantly higher value than that for LDH prepared by other methods. The second maximum is in range of 307–322 °C, where the signals correspond to decomposition of hydromagnesite and dehydroxylation of the interlayer of LDH. Moreover, for hl-Mg/Al-4, a low weight release (4.15 %) is observed at 274 °C. The third maximum is between 441–443 °C, corresponding to the release of CO_2 from decomposition of hydromagnesite, and the fourth between 574–589 °C. On the other hand, the TG curves of hl-reMO are similar to those of reMO prepared by other methods, corresponding to two dominant releases of matter. The first maximum is observed in the range of 167–214 °C, whereas the second between 371–411 °C. For both hl-reMO samples, the peak between 75–107 °C is attributed to an insufficient drying after preparation.

The total weight loss of LDH prepared by the co-precipitation method is in the range of 44–60 %, for related samples of mixed oxides after rehydration (reMO) in the range of 27–57 %. Co-reMO-Mg/Al-3 is the only sample that has a lower weight loss than the parent LDH; co-reMO-Mg/Al-4 revealing a large initial weight loss. The total weight loss of LDH prepared by the sol-gel method is in the range of 53–61 %, for related samples of reMO in the range of 68–86 %. All sg-reMO have a higher total weight loss than that of parent LDH. The total weight loss of LDH prepared by the hydrothermal method is in range 45–48 %, for related samples of reMO in the range of 51–70 %. reMO in all synthesis methods have a higher total weight loss compared to the parent LDH caused by a high content of the weakly bound water after insufficient drying during preparation.
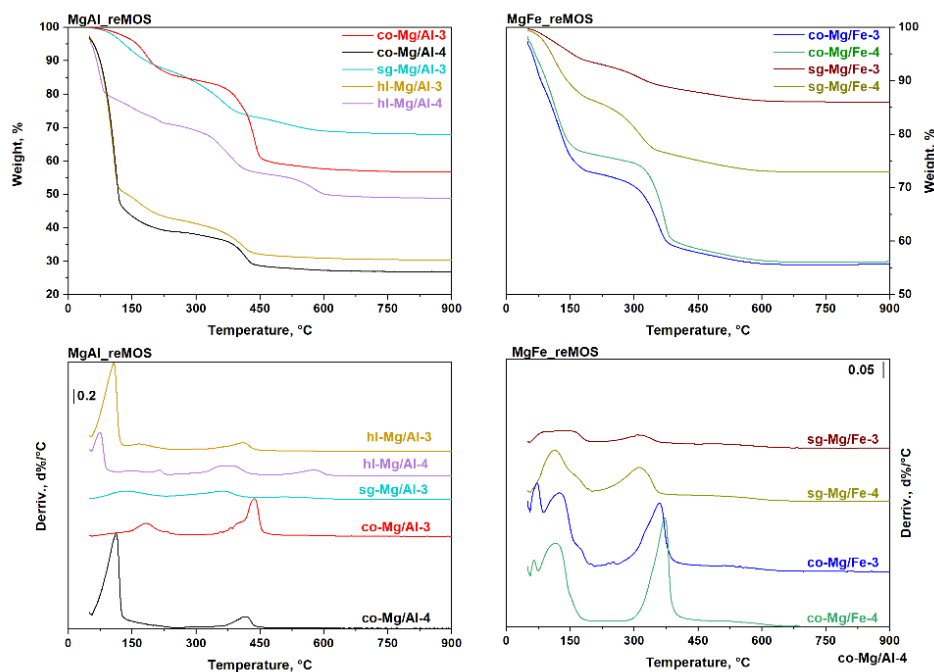
Fig. 5 TGA (up) and dTGA (down) curves of derived reMO

Statistical similarities

To discuss multivariable systems and impact of material synthesis method, we have performed a complex statistical analysis of the results obtained from the LDH and reMO characterization by XRD and TGA. PCA was carried out; the maximal number of treated variables being limited by the number of incoming treated samples. CWP was used to determine the relations between the respective variables: cell parameters *a* and *c*, crystallite sizes *D*, and the mass loss in TG curve for the second step: TGA-2-LDH, TGA-2-reMO. The CWP is displayed in Fig. 6 on the left. The explanation of the CWP: if variables are close to each other, then these variables have a positive correlation. Variables exhibit a negative correlation if they are opposite each other. If the angle between the variables is right, then such variables do not correlate. The scatter plot of scores (SPS) (Fig. 6 on the right) have then provided an insight into how the measured and calculated values contribute to similarity with respect to the differences of samples. Samples from the individual synthetic methods are grouped together, meaning that these methods show statistical similarities. Moreover, the structure properties are influenced neither by the type of trivalent cations (Al or Fe) nor by the molar ratio of the divalent to trivalent ions. It has to be noted that the sample co-Mg/Al-3 is separated from the other samples in the SPS revealing somewhat different structural properties than those of the other analysed samples.

From the PCA analysis presented, several conclusions can be drawn. The cell parameter *a* in the parent LDH strongly correlates with cell parameter *a* in the reMO indicating that the layer properties of the rehydrated MO are very similar to the properties of the parent LDH materials. The cell parameter *a* negatively correlates

with the crystal size D and with the amount of the released matter in the TGA second step (highly pronounced for the parent LDH). It has shown that the increase of the distance among Mg and Al (Fe) in the layer the crystal size and also the amount of the bonded anions in the interlayer layer decreases. It has to be noted that the parameter TG-re-MOS is of lesser importance in the comparison with the others (see Fig. 6 and the point positioned closer to the center of the circle).
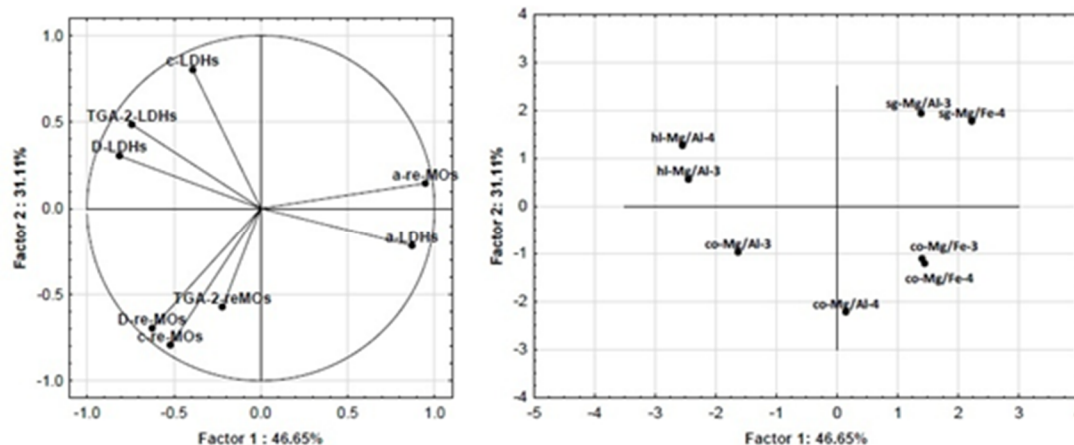

Fig. 6 The component weight plot (CWP) for structural parameters of LDH and reMO (left), and the scatter plot of scores (SPS) (right).

For parent LDH, the cell parameter c, the crystal size D and the second mass release in TGA (TGA-2) are mutually positively correlating parameters. Positive correlation of c, D and TGA-2 is observed also for rehydrated MO. By comparing the parent LDH and reMO, the c, D, and TGA-2 form two separate groups of parameters and thus do not show any correlation in these two forms of materials. In the parent LDH, the compensating anions are carbonates, in rehydrated MO there are hydroxyls as anions in the interlayer. This is mirrored in the value of the interlayer cell parameter c, and related value of crystallite size D. The second step in TG analysis is related to the decomposition of anions and therefore being influenced by the rehydration of material.

Morphology of particles

Crystal structure, morphology of particles, of LDH, MO and reMO were investigated using SEM (Fig.7) to observe the differences among the methods used for synthesis in morphology. For the co-precipitation method, LDH show aggregates with well-ordered thin platelets with hexagonal morphology (see Fig. 7 A and 7 B). The sol-gel method leads to LDH with not well-ordered particles (Fig. 7 C and 7 D). The hydrothermal method leads to LDH with significantly larger particles than those obtained in the other methods; in addition, the particles form aggregates (Fig. 7 E). The formation of the well-ordered LDH particles is influenced mainly by the time and temperature of hydrothermal preparation. After

8 hours at 180 °C, the thin platelets of LDH are formed again as shown before [49], and so prepared materials were used in our study. It was confirmed by XRD, that the crystal size of the hl-LDH is about 3 times larger compared to other methods. The morphology of hydrothermal prepared samples could also be influenced by the presence of hydromagnesite and magnesite phases.
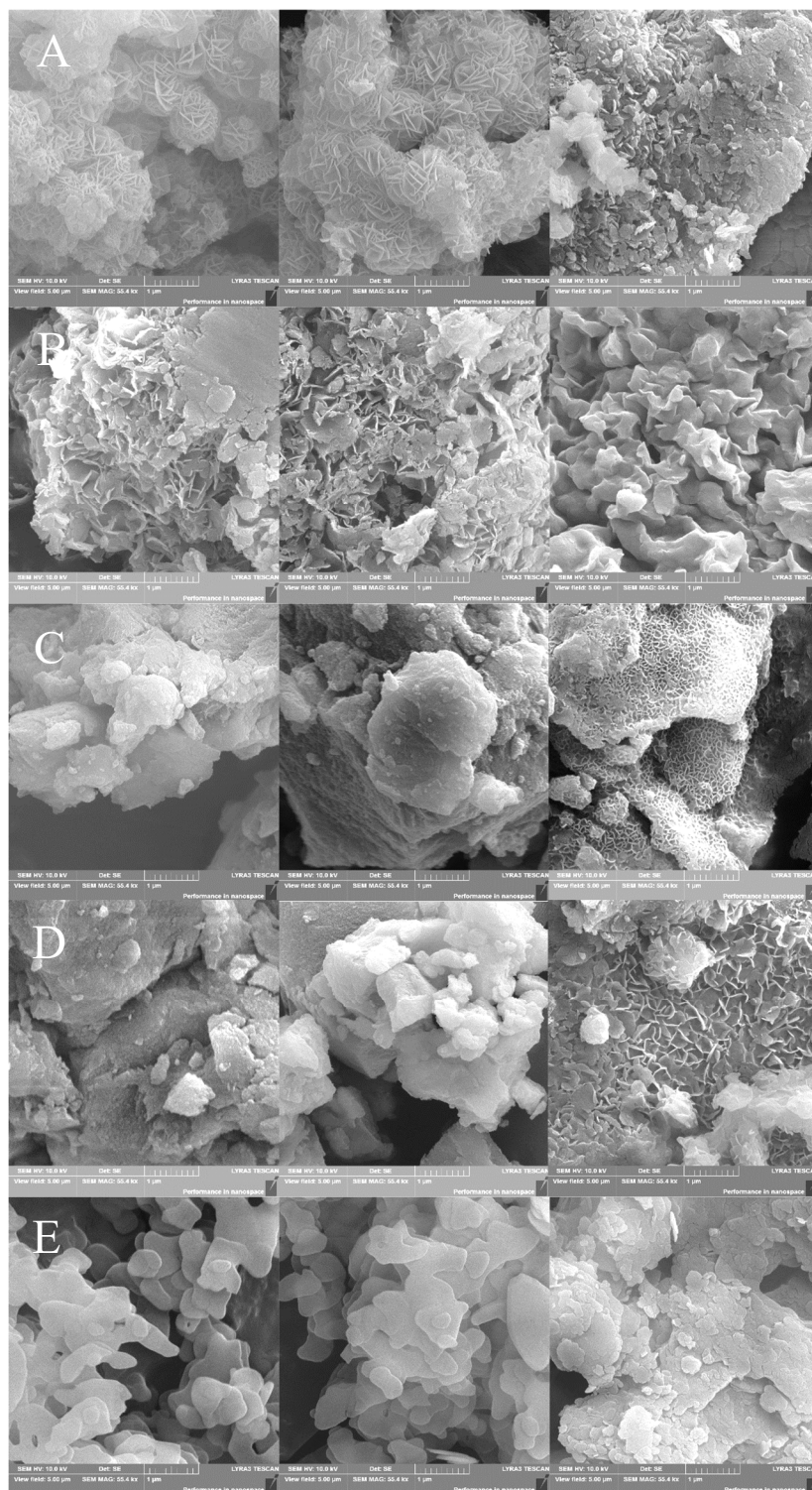
Fig. 7 SEM images of LDH, MO, reMO forms (in order from left) for A) co-Mg/Al-3, B) co Mg/Fe 4, C) sg-Mg/Al-3, D) sg-Mg/Fe-4, and E) hl-Mg/Al-4

The parent LDH, calcined forms (MO), and rehydrated forms (reMO) reveal some differences in the crystal particle structure, in both Mg/Al and Mg/Fe series. The calcination of parent LDH is connected with small changes in the crystal structure. The rehydration of MO had a greater influence in morphological changes than the calcination. For the samples prepared by co-precipitation, the structure looks similar before and after calcination, it is a developed crystal structure. After rehydration, the original "leaf" crystal structure changes to larger "scale" particles. The presence of pure LDH phase in rehydrated samples from co-precipitation was confirmed by XRD. In the case of sol-gel method, the original LDH and MO show a not very developed crystalline structure, however, after rehydration a leaf structure characteristic of LDH can be observed. It should be noted that sg-reMO are only partially rehydrated to the LDH, additional phase of MgO is observed.

In the hydrothermal method, the rehydration leads to the formation of smaller crystallites with the similar morphology to the parent and calcined forms, which is in accordance with the XRD results. The hl-reMO exhibits also the higher amount of LDH phase compared to the parent form.

Textural properties

The effect of synthesis method of parent LDH materials and chemical composition on the textural properties of resulting MO forms has been studied. The adsorption isotherms of MO were determined and pore-size distribution was calculated (Fig. 8), together with the specific surface area evaluated by the BET method (Table 5).

The adsorption isotherms of the MO from co-precipitation method (both Mg/Al and Mg/Fe) correspond to the isotherm type IV with the hysteresis loop type H3, which is typical for clay materials, showing the slit-shaped pores situated between the aggregates of platelets. On the other hand, isotherms of the MO from sol-gel method correspond to the isotherm type IV with the hysteresis loop type H2. The difference in the shape of pores is caused by the gelling agent, whereas the exchange of the capillary forces and shrinkage are due to replacement the water by the alcohols during the sol-gel synthesis of LDH [35,50]. This leads to the ink-bottle shaped pores or the variable cylindrical structures that have intersect with each other, thus creating a larger free volume at the point of intersection. Isotherms of the MO from hydrothermal synthesis correspond to the isotherm type IV and show a very small hysteresis loop, suggesting a small contribution of capillary condensation.

The pore-size distribution of MO is also dependent on the type of synthesis. All MO have the maximum on the distribution curve in the range of mesopores, the MO-Mg/Al mixed oxides possess the pores with smaller sizes than MO-Mg/Fe. MO from co-precipitation and hydrothermal syntheses then exhibits additional contribution in the range of micropores. Co-precipitation method leads to a MO with wide distribution of pore sizes. For co-MO-Mg/Al, the pore-size range from

1 to 50 nm with the abundance of pores 4–5 nm. For co-MO-Mg/Fe, the pore sizes range from 3 to 50 nm with the abundance of pores 6–7 nm. On the other hand, sol-gel method leads to MO with relatively narrow pore size distribution, with maximum at 5–6 nm for sg-MO-Mg/Al and 8–9 nm for sg-MO-Mg/Fe. For hydrothermal synthesis, the distribution of pore sizes is in the range of 1–10 nm, with maximum around 3–6 nm. It should be noted that the Mg^{2+}/Me^{3+} molar ratio also affects the position of the maximum on the distribution curve (for both Mg/Al and Mg/Fe series). MO with a ratio of $Mg^{2+}/Me^{3+} = 4$ have the maximum shifted to higher sizes compared to the structure with the ratio = 3. For sol-gel prepared MO-Mg-Al with a Mg/Al molar ratio = 2, it was previously observed that the maximum on the distribution curve is localized at around 4 nm [50], being slightly lower in the comparison with our MO, thus demonstrating the effect Mg^{2+}/Me^{3+} ratio.

The specific surface area of MO is in the range 122–229 m^2 g^{-1}. Comparable S(BET) values are detected for co-precipitation and sol-gel syntheses (in the respective samples with the same composition). Significantly lower S(BET) values are then detected for MO from hydrothermal synthesis. Differences are observed between Mg/Al and Mg/Fe series; Mg/Al MO show higher specific surfaces than Mg/Fe MO, after calcination, Mg/Al MO attains the specific surface area between 219–225 m^2 g^{-1}, while specific surface area of Mg/Fe MO is between 122–145 m^2 g^{-1}. This goes in parallel with our previous results with various Mg/Al and Mg/Fe mixed oxides [16,19]. In addition, the Mg^{2+}/Me^{3+} molar ratios = 4 show specific surface areas of about 4–20 % higher compared to the ratios = 3, including both Mg/Al and Mg/Fe MO series.
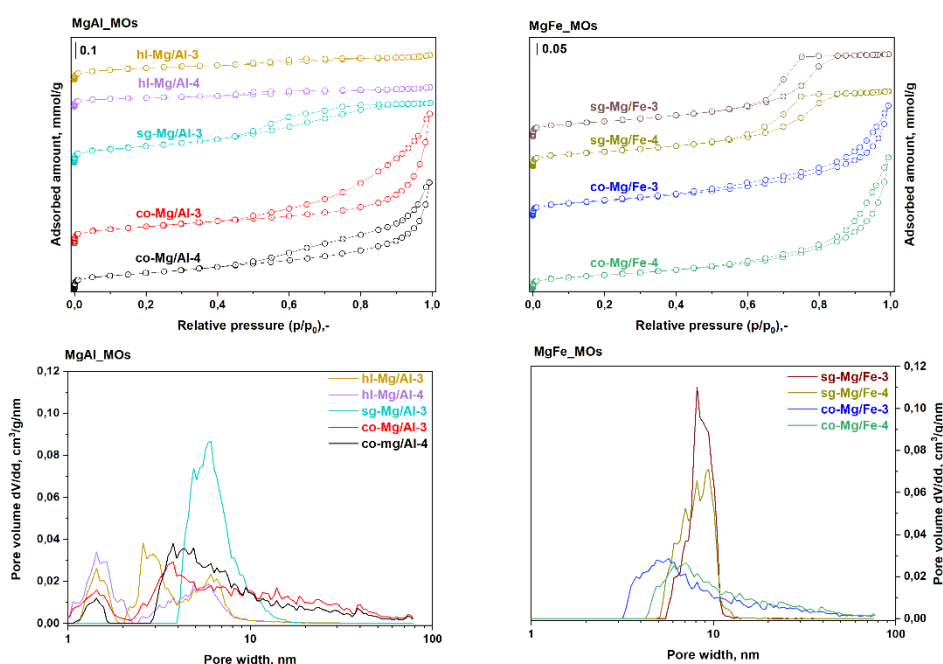
Fig. 8 MO forms and N_2 adsorption isotherms (upper plots) and pore size distribution curves (on bottom)

Table 5 Specific surface area and acid-base properties of co-MO, sg-MO and hl-MO

Sample	Specific surface area S (BET)	Basic centres		Acid centres	
		Concentration	Density	Concentration	Density
	[$m^2\ g^{-1}$]	[$\mu mol\ g^{-1}$]	[$\mu mol\ m^{-2}$]	[$\mu mol\ g^{-1}$]	[$\mu mol\ m^{-2}$]
co-Mg/Al-3	229	204	0.89	163	0.71
co-Mg/Al-4	219	205	0.94	132	0.60
co-Mg/Fe-3	144	134	0.93	116	0.80
co-Mg/Fe-4	122	169	1.38	108	0.88
sg-Mg/Al-3	225	220	0.98	185	0.82
sg-Mg/Fe-3	145	135	0.93	149	1.03
sg-Mg/Fe-4	139	152	1.09	141	1.01
hl-Mg/Al-3	149	328	2.20	158	1.06
hl-Mg/Al-4	124	243	1.96	97	0.78

Acid-base properties

Basic and acid properties of MO forms have been studied using temperature programmed desorption of carbon dioxide (CO_2-TPD) and ammonia (NH_3-TPD), respectively. The resultant CO_2-TPD curves are depicted in Fig. 9 A (Mg/Al) and B (Mg/Fe), and NH_3-TPD curves in Fig. 9 C (Mg/Al) and D (Mg/Fe). The total number of basic and acid sites was determined from the area under the signal curve from the MS detector (reduced mass 44/4 for CO_2-TPD and 16/4 for NH_3-TPD) corresponding to the total amount of carbon dioxide desorbed in the temperature range of 35–450 °C and ammonia in the range of 70–450 °C, respectively (Table 5). For some applications, namely catalysis, it is relevant to discuss the surface density of centres and the amount of centres related to the specific surface area (Table 5).

For both MO-Mg/Al and Mg/Fe series, only small nuances in the concentrations and densities of basic centres were observed between the co-precipitation and sol-gel synthesis methods. However, samples of hydrothermally prepared MO-Mg/Al showed significantly more basic centres and higher densities than other synthesized MO-Mg/Al. It can be concluded that hydrothermal method relates to surface defects lead to the abundance of basic centres.

The studied MO-Mg/Al and MO-Mg/Fe series differ significantly in the total basicity. MO-Mg/Al have a higher number of basic centres, both in the co-precipitation and sol-gel methods, than MO-Mg/Fe. This observation is in line with our previous studies on various Mg/Al and Mg/Fe mixed oxides [16,19]. However, when the basicity is expressed as density of centres, MO-Mg/Fe exhibits a slightly higher density than MO-Mg/Al due to the lower specific surface area of MO-Mg/Fe.

The measured CO_2-TPD curves peaked at around 110 °C and they are tailed at high temperature side. From the shape of the desorption CO_2-TPD curve, it can be concluded that the samples contain a wide distribution of basic centres. First, carbon dioxide bound into weak basic centres (approx. 110 °C) is released, then followed by that from medium-strength basic centres (approx. 170 °C) and from strong basic centres (approx. 270 °C) [16,18,24]. On the TPD curves obtained, a maximum is observable at a temperature of 100–110 °C, which is characteristic for weak basic centres. Yet another local maximum around 260 °C is clearly observed for most samples, corresponding to strong basic centres.

When considering the distribution of basic centres, there are several differences among synthesis methods (insets Figure 9 A and B). For MO-Mg/Al, samples prepared by hydrothermal method reveal higher population of medium-strength and strong basic centres. A sample originated from sol-gel method reveals the highest population of weak basic centres. Similarly, for MO-Mg/Fe, higher population of weak basic centres is expressed by the samples having originated from sol-gel method. Hydrothermal synthesis led to the most heterogeneous LDH samples (more crystallographic phases), so it is possible to conclude that the most surface defects (unsaturated oxygens on the surface) leading to a higher population of medium and strong basic centres are present at the related MO.

Acid properties are dependent on the synthesis method. For both MO-Mg/Al and MO-Mg/Fe series, samples prepared by sol-gel method show somewhat higher total amount and density of acid centres.

The studied MO-Mg/Al and Mg/Fe series differ in the total acidity. MO-Mg/Al have a higher number of acid centres, both in the co-precipitation and sol-gel methods, than MO-Mg/Fe. However, MO-Mg/Fe show somewhat higher density of acid centres than that at MO-Mg/Al.

The measured NH_3-TPD curves peaked at around 170 °C. All curves are tailed at the high temperature side, due to the presence of several types of NH_3 complexes on acid centres (insets Figure 9 C and D). No major differences in the acid centre distribution could be observed for the synthesis methods. Nevertheless, the extent of the high temperature tail depends on the oxide composition – MO-Mg/Fe series contain a slightly higher population at high temperature than MO-Mg/Al series, thus mirroring the presence of relatively stronger acid centres on the Mg/Fe oxide surface.
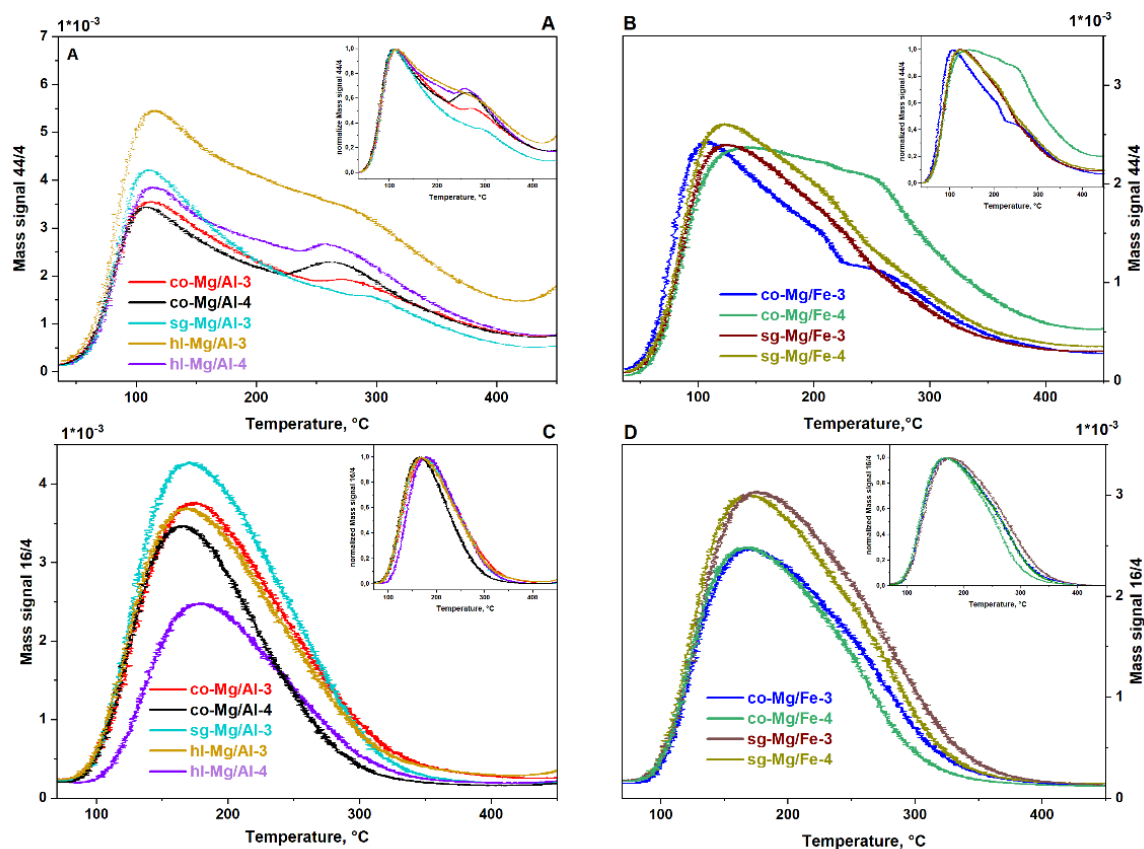
Fig. 9 CO_2-TPD curves for Mg/Al (A) and Mg/Fe (B) MO, resp., and NH_3-TPD curves for Mg/Al (C) and Mg/Fe (D) MO, resp.

Conclusions

The co-precipitation, sol-gel and hydrothermal methods previously widely used for synthesis of MgAl LDH have been applied in the synthesis of MgFe LDH with the theoretical metal molar ratios of 3/1 and 4/1; the properties of MgAl and MgFe being investigated in detail. Certain similarities of material characteristics for particular synthesis were observed, when the co-precipitation method resulted in samples with the composition closest to the target values. The highest deviations in the metal ratio were noticed for the hydrothermally prepared LDH. Samples prepared by the co-precipitation and sol-gel method were pure hydrotalcite-like phases. On the other hand, MgAl samples from the hydrothermal method were found to contain additional phases. Nevertheless, Mg/Fe LDH from the hydrothermal method could not be successfully prepared and remain a challenge for the future work.

In the statistical analysis of the structural data, the samples from particular synthesis method had been grouped together, which means that the respective samples exhibited statistical similarities. It has been shown that the structure properties of samples from particular synthesis are similar for both series of Mg/Al and Mg/Fe and also for the molar metal ratios 3/1 and 4/1.

The hydrothermal method led to the LDH with the highest values of crystallite sizes (60–70 nm). Co-precipitation and sol-gel method gave rise to the significantly lower crystallite sizes, 10–15 nm (co-LDH) and 9–10 nm (sg-LDH). For the co-precipitation method, LDH showed aggregates with well-ordered thin platelets with hexagonal morphology. The sol-gel method led to LDH with not well-ordered particles. The hydrothermal method resulted in the LDH with significantly larger particles than those obtainable by the other methods; moreover, such particles formed aggregates.

The rehydration of the MO revealed that co-precipitated samples could be completely rehydrated back to the LDH; however, for sol-gel prepared samples the rehydration was not complete. Hydrothermally prepared samples were originally heterogeneous and were not completely rehydrated to the LDH form. The cell parameter *a* in the parent LDH strongly correlated with cell parameter *a* in the rehydrated forms indicating that the layer properties of rehydrated forms had been very similar to the properties of parent LDH materials. It was showed that with the increase of the distance among Mg and Al (Fe) in the layer the crystal size and, also, the amount of the bonded anions in the interlayer layer decreased. For parent LDH, and separately also for rehydrated forms, the cell parameter *c*, the crystal size *D,* and the second mass release in TGA were mutually positively correlating parameters.

Only small differences in the total number and densities of basic centres on the surface of mixed oxide forms were observed between the co-precipitation and sol-gel synthesis methods, for both Mg/Al and Mg/Fe series. However, Mg/Al oxides originated from hydrothermal LDH showed significantly more basic centres and higher densities than the other mixed oxides, due to the abundance of surface defects and other phases. Additionally, oxides from the hydrothermal method revealed a higher population of medium-strength and strong basic centres. Sample originating from the sol-gel method revealed the highest population of weak basic centres. In parallel, acid properties were also dependent on the synthesis method. For both Mg/Al and Mg/Fe series, oxides prepared by the sol-gel method showed somewhat higher total amount and density of acid centres.

References

[1]   Sels B.F., De Vos D.E., Jacobs P.A.: Hydrotalcite-like anionic clays in catalytic organic reactions. *Catalysis Reviews* **43** (2001) 443–488.

[2]   Xu Z.P., Zhang J., Adebajo M.O., Zhang H., Zhou C.: Catalytic applications of layered double hydroxides and derivatives. *Applied Clay Science* **53** (2011) 139–150.

[3]   Kaneda K., Mizugaki T.: Design of high-performance heterogeneous catalysts using hydrotalcite for selective organic transformations. *Green Chemistry* **21** (2019) 1361–1389.

[4]   Fan G., Li F., Evans D.G., Duan X.: Catalytic applications of layered double hydroxides: recent advances and perspectives. *Chemical Society Reviews* **43** (2014) 7040–7066.

[5]   Cavani F., Trifirò F., Vaccari A.: Hydrotalcite-type anionic clays: Preparation, properties and applications. *Catalysis Today* **11** (1991) 173–301.

[6]   Tian R., Liang R., Wei M., Evans D.G., Duan X.: Applications of layered double hydroxide materials: Recent advances and perspective, in: Mingos D.M.P. (Ed.): *50 years of structure and bonding – The anniversary volume*, Springer International Publishing, Cham 2017, pp 65–84.

[7]   Abelló S., Medina F., Tichit D., Pérez-Ramírez J., Sueiras J.E., Salagre P., Cesteros Y.: Aldol condensation of campholenic aldehyde and MEK over activated hydrotalcites. *Applied Catalysis B: Environmental* **70** (2007) 577–584.

[8]   Kikhtyanin O., Tišler Z., Velvarská R., Kubička D.: Reconstructed Mg-Al hydrotalcites prepared by using different rehydration and drying time: Physico-chemical properties and catalytic performance in aldol condensation. *Applied Catalysis A: General* **536** (2017) 85–96.

[9]   Ordóñez S., Díaz E., Leon M., Faba L.: Hydrotalcite-derived mixed oxides as catalysts for different C–C bond formation reactions from bioorganic materials. *Catalysis Today* **167** (2011) 71–76.

[10]   Faba L., Díaz E., Ordóñez S.: Aqueous-phase furfural-acetone aldol condensation over basic mixed oxides. *Applied Catalysis B: Environmental* **113–114** (2012) 201–211.

[11]   Prado R.G., de Almeida G.D., de O. Carvalho M.M., Galvão L.M., Bejan C.C.C., da Costa L.M., Pinto F.G., Tronto J., Pasa V.M.D.: Multivariate method for transesterification reaction of soybean oil using calcined Mg-Al layered double hydroxide as catalyst. *Catalysis Letters* **144** (2014) 1062–1073.

[12]   Zeng H.-Y., Xu S., Liao M.-C., Zhang Z.-Q., Zhao C.: Activation of reconstructed Mg/Al hydrotalcites in the transesterification of microalgae oil. *Applied Clay Science* **91–92** (2014) 16–24.

[13]   Hora L., Kelbichová V., Kikhtyanin O., Bortnovskiy O., Kubička D.: Aldol condensation of furfural and acetone over MgAl layered double hydroxides and mixed oxides. *Catalysis Today* **223** (2014) 138–147.

[14]   Hora L., Kikhtyanin O., Čapek L., Bortnovskiy O., Kubička D.: Comparative study of physico-chemical properties of laboratory and industrially prepared layered double hydroxides and their behavior in aldol condensation of furfural and acetone. *Catalysis Today* **241** (2015) 221–230.

[15]   Smoláková L., Frolich K., Kocík J., Kikhtyanin O., Čapek L.: Surface properties of hydrotalcite-based Zn(Mg)Al oxides and their catalytic activity in aldol condensation of furfural with acetone. *Industrial & Engineering Chemistry Research* **56** (2017) 4638–4648.

[16]   Hájek M., Kocík J., Frolich K., Vávra A.: Mg-Fe mixed oxides and their rehydrated mixed oxides as catalysts for transesterification. *Journal of Cleaner Production* **161** (2017) 1423–1431.

[17]   Kikhtyanin O., Čapek L., Smoláková L., Tišler Z., Kadlec D., Lhotka M., Diblíková P., Kubička D.: Influence of Mg–Al mixed oxide compositions on their properties and performance in aldol condensation. *Industrial & Engineering Chemistry Research* **56** (2017) 13411–13422.

[18]   Kocík J., Frolich K., Perková I., Horáček J.: Pyroaurite-based Mg-Fe mixed oxides and their activity in aldol condensation of furfural with acetone: Effect of oxide composition. *Journal of Chemical Technology & Biotechnology* **94** (2019) 435–445.

[19] Lima-Corrêa R.A.B., Castro C.S., Damasceno A.S., Assaf J.M.: The enhanced activity of base metal modified MgAl mixed oxides from sol-gel hydrotalcite for ethylic transesterification. *Renewable Energy* **146** (2020) 1984–1990.

[20] Taylor H.F.W.: Crystal structures of some double hydroxide minerals. *Mineralogical Magazine* **39** (1973) 377–389.

[21] Vaccari A.: Clays and catalysis: A promising future. *Applied Clay Science* **14** (1999) 161–198.

[22] Khan A.I., O'Hare D.: Intercalation chemistry of layered double hydroxides: Recent developments and applications. *Journal of Materials Chemistry* **12** (2002) 3191–3198.

[23] Williams G.R., O'Hare D.: Towards understanding, control and application of layered double hydroxide chemistry. *Journal of Materials Chemistry* **16** (2006) 3065–3074.

[24] Di Cosimo J.I., Díez V.K., Xu M., Iglesia E., Apesteguía C.R.: Structure and surface and catalytic properties of Mg-Al basic oxides. *Journal of Catalysis* **178** (1998) 499–510.

[25] Prinetto F., Ghiotti G., Durand R., Tichit D.: Investigation of acid−base properties of catalysts obtained from layered double hydroxides. *The Journal of Physical Chemistry B* **104** (2000) 11117–11126.

[26] Hibino T., Tsunashima A.: Calcination and rehydration behavior of Mg-Fe-CO_3 hydrotalcite-like compounds. *Journal of Materials Science Letters* **19** (2000) 1403–1405.

[27] Kuśtrowski P., Sułkowska D., Chmielarz L., Olszewski P., Rafalska-Łasocha A., Dziembaj R.: Effect of rehydration conditions on the catalytic activity of hydrotalcite-derived Mg-Al oxides in aldolization of acetone. *Reaction Kinetics and Catalysis Letters* **85** (2005) 383–390.

[28] Xu C., Gao Y., Liu X., Xin R., Wang Z.: Hydrotalcite reconstructed by in situ rehydration as a highly active solid base catalyst and its application in aldol condensations. *RSC Advances* **3** (2013) 793–801.

[29] Panda H.S., Srivastava R., Bahadur D.: Synthesis and in situ mechanism of nuclei growth of layered double hydroxides. *Bulletin of Materials Science* **34** (2011) 1599–1604.

[30] Zhang L., Zhu J., Jiang X., Evans D.G., Li F.: Influence of nature of precursors on the formation and structure of Cu-Ni-Cr mixed oxides from layered double hydroxides. *Journal of Physics and Chemistry of Solids* **67** (2006) 1678–1686.

[31] Olanrewaju J., Newalkar B.L., Mancino C., Komarneni S.: Simplified synthesis of nitrate form of layered double hydroxide. *Materials Letters* **45** (2000) 307–310.

[32] Álvarez M.G., Chimentão R.J., Figueras F., Medina F.: Tunable basic and textural properties of hydrotalcite derived materials for transesterification of glycerol. *Applied Clay Science* **58** (2012) 16–24.

[33] Sharma U., Tyagi B., Jasra R. V.: Synthesis and characterization of Mg-Al-CO_3 layered double hydroxide for CO_2 adsorption. *Industrial & Engineering Chemistry Research* **47** (2008) 9588–9595.

[34] Aramendia M., Borau V., Jiménez C., Marinas J.M., Ruiz J.R., Urbano F.J.: Comparative study of Mg/*M*(III) (*M* = Al, Ga, In) layered double hydroxides obtained by coprecipitation and the sol-gel method. *Journal of Solid State Chemistry* **168** (2002) 156–161.

[35] Prinetto F., Ghiotti G., Graffin P., Tichit D.: Synthesis and characterization of sol-gel Mg/Al and Ni/Al layered double hydroxides and comparison with co-precipitated samples. *Microporous and Mesoporous Materials* **39** (2000) 229–247.

[36] Olsbye U., Akporiaye D., Rytter E., Rønnekleiv M., Tangstad E.: On the stability of mixed M^{2+}/M^{3+} oxides. *Applied Catalysis A: General* **224** (2002) 39–49.

[37] Rao M.M., Reddy B.R., Jayalakshmi M., Jaya V.S., Sridhar B.: Hydrothermal synthesis of Mg-Al hydrotalcites by urea hydrolysis. *Materials Research Bulletin* **40** (2005) 347–359.

[38] Kovanda F., Grygar T., Dorničák V., Rojka T., Bezdička P., Jirátová K.: Thermal behaviour of Cu-Mg-Mn and Ni-Mg-Mn layered double hydroxides and characterization of formed oxides. *Applied Clay Science* **28** (2005) 121–136.

[39] Yang Z., Zhou H., Zhang J., Cao W.: Relationship between Al/Mg ratio and the stability of single-layer hydrotalcite. *Acta Physico-Chimica Sinica* **23** (2007) 795–800.

[40] Elmoubarki R., Mahjoubi F.Z., Elhalil A., Tounsadi H., Abdennouri M., Sadiq, M., Qourzal S., Zouhri A., Barka N.: Ni/Fe and Mg/Fe layered double hydroxides and their calcined derivatives: preparation, characterization and application on textile dyes removal. *Journal of Materials Research and Technology* **6** (2017) 271–283.

[41] Ogawa M., Kaiho H.: Homogeneous precipitation of uniform hydrotalcite particles. *Langmuir* **18** (2002) 4240–4242.

[42] Oh J.-M., Hwang S.-H., Choy J.-H.: The effect of synthetic conditions on tailoring the size of hydrotalcite particles. *Solid State Ionics* **151** (2002) 285–291.

[43] Tampieri A., Lilic M., Constantí M., Medina F.: Microwave-assisted aldol condensation of furfural and acetone over Mg-Al hydrotalcite-based catalysts. *Crystals* **10** (2020) 833.

[44] Kocík J., Hájek M., Tišler Z., Strejcová K., Velvarská R., Bábelová M.: The influence of long-term exposure of Mg-Al mixed oxide at ambient conditions on its transition to hydrotalcite. *Journal of Solid State Chemistry* **304** (2021) 122556.

[45] Mück J., Kocík J., Hájek M., Tišler Z., Frolich K., Kašpárek A.: Transition metals promoting Mg-Al mixed oxides for conversion of ethanol to butanol and other valuable products: Reaction pathways. *Applied Catalysis A: General* **626** (2021) 118380.

[46] Kowalewski E., Krawczyk M., Słowik G., Kocik J., Pieta I.S., Chernyayeva O., Lisovytskiy D., Matus K., Śrębowata A.: Continuous-flow hydrogenation of nitrocyclohexane toward value-added products with CuZnAl hydrotalcite derived materials. *Applied Catalysis A: General* **618** (2021) 118134.

[47] Labuschagné F.J.W.J., Wiid A., Venter H.P., Gevers B.R., Leuteritz A.: Green synthesis of hydrotalcite from untreated magnesium oxide and aluminum hydroxide. *Green Chemistry Letters and Reviews* **11** (2018) 18–28.

[48] Kovanda F., Koloušek D., Cílová Z., Hulínský V.: Crystallization of synthetic hydrotalcite under hydrothermal conditions. *Applied Clay Science* **28** (2005) 101–109.

[49] Bolognini M., Cavani F., Scagliarini D., Flego C., Perego C., Saba M.: Mg/Al mixed oxides prepared by coprecipitation and sol-gel routes: A comparison of their physico-chemical features and performances in *m*-cresol methylation. *Microporous and Mesoporous Materials* **66** (2003) 77–89.

[50] Lavalley J.C.: Infrared spectrometric studies of the surface basicity of metal oxides and zeolites using adsorbed probe molecules. *Catalysis Today* **27** (1996) 377–401.